

AD-A047 957

ILLINOIS UNIV AT URBANA-CHAMPAIGN DEPT OF METALLURGY --ETC F/6 11/6
HYDROGEN EMBRITTLEMENT OF NIOBIUM III - HIGH TEMPERATURE BEHAVI--ETC(U)
OCT 77 S GAHR, H K BIRNBAUM

UNCLASSIFIED

N00014-75-C-1012

NL

| OF |

AD
A047957



END

DATE
FILMED

1 -78

DDC

AD A 047957

(10)

HYDROGEN EMBRITTLEMENT OF NIOBIUM III -
HIGH TEMPERATURE BEHAVIOR

S. Gahr and H. K. Birnbaum

(See back page
for 14713)

Technical Report
Office of Naval Research Contract N 00014-75-C-1012
October 18, 1977

University of Illinois at Urbana-Champaign
Department of Metallurgy and Mining Engineering
Urbana, Illinois 61801

DDC
RECEIVED
DEC 22 1977
F

This document is unclassified. Distribution and reproduction for any purpose of the U. S. government is permitted.

AD No. _____
DDC FILE COPY

DISTRIBUTION STATEMENT A
Approved for public release;
Distribution Unlimited

ABSTRACT

The deformation behavior of niobium - hydrogen alloys was investigated in the temperature range 125-500 C and at compositions up to H/Nb of 0.9. High temperature tensile tests and fractographic studies were applied to determine the fracture mechanisms. It is shown that at $T \lesssim 450^{\circ}\text{C}$ and $\text{H/Nb} \gtrsim 0.3$ fracture occurs by a cleavage mode. The mechanism of this high temperature hydrogen embrittlement is discussed. The fracture mechanism is shown to be consistent with the stress induced formation and cleavage of NbH_2 .

ACCESSION for	
NTIS	in the Section <input checked="" type="checkbox"/>
DDC	in the Section <input type="checkbox"/>
UNCLASSIFIED	<input type="checkbox"/>
JUL 1 1961 <i>on file</i>	
BY	
DISTRIBUTION/AVAILABILITY CODES	
Dist.	Class
A	

1. INTRODUCTION

The effect of hydrogen on the low temperature mechanical properties and fracture of the Group vb transition metals has been extensively reported in the literature (1). Experimental studies have generally been carried out in a temperature and composition range where the solubility of hydrogen is limited by the precipitation of a hydride phase in equilibrium with the solid solution. In two previous publications (2,3) it has been shown the hydrogen embrittlement in the Nb-H system under these conditions is caused by precipitation and cleavage of a stress induced brittle hydride. It was also demonstrated that the Nb-H solid solution is inherently ductile and fails in a ductile mode unless stress induced brittle hydride formation intervenes.

Few studies (4) of the effect of hydrogen on mechanical properties have been carried out at elevated temperatures and high hydrogen concentrations where hydrides are not considered to be stable. The present paper reports the results of such a study in the Nb-H system at temperatures in the range 130 C to 500 C and at hydrogen concentrations as high as $H/Nb = 0.93$. The Nb-H phase diagram (5) indicates that this region of the phase diagram corresponds to a solid solution, α' .

2. EXPERIMENTAL PROCEDURE

Tensile specimens having a gage length of 1.8 cm and a width of 0.5 cm were machined from 0.1 cm thick polycrystalline Nb sheet. They were given a high temperature anneal at 2000 C at 5.3×10^{-4} Pa (4×10^{-6} torr) which produced an average grain

size of about 0.3 cm and the impurity concentrations given in Table I. Hydrogen concentrations were determined by vacuum extraction and by weighing after tensile testing.

Hydrogen charging was performed in-situ in a UHV tensile furnace mounted on an Instron testing machine. This allowed tensile testing in the temperature range 20-1000 C in a hydrogen atmosphere whose pressure was equilibrated with the desired composition and without cooling through phase boundaries. After evacuation to 1×10^{-6} Pa (5×10^{-9} torr) hydrogen, which was purified by diffusion through a Pd-Ag membrane, was introduced and the specimen was heated. The hydrogen pressure was adjusted to maintain the desired H/Nb during tensile testing and during cooling after testing. Test temperatures were controlled to ± 0.5 C using a Pt-Pt 13% Rh thermocouple mounted next to the specimen. The tensile parameters were obtained from the Instron chart recording with the strain to failure. The strain to failure, ϵ_f , was defined as the tensile elongation to fracture and, the yield stress was defined by the deviation from the elastic loading line.

3. EXPERIMENTAL RESULTS

The general fracture behavior of the high concentration Nb-H alloys is shown in Fig. 1 as a function of H/Nb and temperature. Below about 300 C a relatively temperature insensitive ductile to cleavage fracture transition is observed at a critical hydrogen concentration of $H/Nb \approx 0.3$. At higher temperatures a higher concentration is required to cause cleavage fracture while at $T \gtrsim 450$ C a completely ductile

Table I
Analysis of Niobium Specimens

Impurity Solute	Concentration†(at. ppm)
S	4.0
Ti	0.1
V	0.2
Cr	0.04
Mn	0.03
Fe	0.03
Cu	0.1
Zn	0.06
Zr	0.06
Mo	0.4
Ta	10.0
W	5.0
O	63-140
N	330-465
C	40-90

†Metallic impurity levels were determined by mass spectrometer analysis. O, N and C levels were determined by vacuum fusion methods.

fracture behavior is observed for hydrogen concentrations as high as $H/Nb = 0.87$.

The macroscopic strain to failure decreases as the H/Nb increases and as the temperature decreases as shown in Fig. 1. Alloys within the region indicated by "cleavage" fail by a cleavage mode despite the high macroscopic ductility observed for alloys near the "ductile-cleavage" boundary. The transition in the fracture mode is quite abrupt as evidenced by the change in fracture mode which results from only a small increase in H/Nb or decrease in temperature (Fig. 1). A few Nb-D alloys were tested (Fig. 1) with results similar to those observed for the Nb-H alloys. Similarly, alloys prepared from heavily cold rolled Nb sheet exhibit the same types of fracture behavior as the annealed specimens (Fig. 1) despite the much higher macroscopic fracture stresses.

In a number of respects the hydrogen related fractures at high temperature are similar to those observed at low temperatures. In particular, the observation of cleavage fracture in alloys which exhibit large values of strain to failure is noted. The dependence of the fracture mode on H/Nb at 300 C is shown in Fig. 2. Figure 2a illustrates the ductile fracture mode and complete "necking" to 100% R.A. which is characteristic of specimens having concentrations $H/Nb \lesssim 0.26$. Slightly increasing the hydrogen concentration to $H/Nb = 0.30$ causes a marked change in the fracture mode to cleavage (Fig. 2b) despite the 18% strain to failure. At

hydrogen concentrations of $H/Nb = 0.7$ and $H/Nb = 0.93$ (Figs. 2c and 2d) the failure mode is cleavage and the macroscopic strain to failure is greatly decreased (to $\lesssim 1\%$).

The cleavage - ductile fracture transition on increasing the temperature is also abrupt as illustrated in Figs. 1 and 3 for $H/Nb = 0.7$. Increasing the temperature from 130 C to 300 C had little effect on the macroscopic strain ($\sim 1\%$) or on the microscopic fracture behavior, the failure mode being cleavage (Figs. 3a-d). On further increasing the temperature to 400 C, the macroscopic strain to failure was increased to 5.4%, although the fracture mode remained cleavage (3e). Increasing the temperature to 450 C leads to a complete return of ductility in both macroscopic strain and in microscopic failure mode (Fig. 3f) as the specimen fails by ductile necking.

Fractographic studies indicate that crack propagation occurs transgranularly along the $\{110\}$ (referred to the b.c.c. α' unit cell). When the $\{110\}$ fracture plane is approximately normal to the tension axis the fracture surfaces are quite flat and planar (Figs. 2c and 3b and d) while more highly faceted cleavage is observed for less favorably inclined $\{110\}$ planes (Fig. 3c and e). The appearance of "splinters" and secondary cracking on fracture surfaces is similar to that observed in low temperature fracture of Nb-H alloys (2,3) and is consistent with fracture through brittle phases of appreciable thickness.

The fracture surface energy of oriented single crystal specimens having $H/Nb = 0.81$ and tested at 138 C was determined

for both the $\{110\}$ and $\{100\}$ fracture planes. The crystals were tested in three point bending with the maximum tensile stress being perpendicular to the desired fracture plane. The specimens were pre-cracked using a spark discharge technique and the values of the critical stress intensity factor and the surface energy γ_{eff} shown in Table II were determined using linear elastic fracture mechanics. The $\{110\}_c$ cleavage surface was planar while the $\{100\}_c$ was highly faceted as shown in Fig. 4. The cleavage fractures were not accompanied significant deformation as indicated by the electron channel patterns (Figs. 4c and d) obtained from the cleavage surfaces. These patterns, which were obtained using 200kV electrons, are indicative of plastic strain being less than about 2% within 1000 Å of the cleavage surface. The values for the $\{100\}$ cleavage surface energies are high, in part due to the highly faceted surface and the concomitant underestimate of the surface area.

4. DISCUSSION

A number of mechanisms have been proposed to account for hydrogen embrittlement. In hydrogen solid solutions, a "lattice decohesion" model based on the concept that hydrogen lowers the "cohesive energy" of the metal matrix has been suggested by Troiano and developed by Oriani (7,8). This postulated decrease in the strength of the atomic bonding due to hydrogen is consistent with our observation of a sharp ductile - cleavage transition at about $H/Nb \approx 0.30$. The mechanism is however in direct contradiction to the measured cleavage surface energies about 10.8 J/m^2 for the observed $\{110\}$ fracture plane.

Table II Effective Fracture Surface Energies

Cleavage Plane	γ_{Eff} (J/m ²)
{110}	10.8 \pm 0.5
{100}	32.2 \pm 0.7

This value of the surface energy is in the range normally expected for b.c.c. metals in the absence of hydrogen^(9,10) and suggests that no significant reduction of surface energy occurs even at the very high H/Nb alloys tested.

The conclusion that atomic bonding is not reduced by H in solid solution is supported by recent neutron scattering measurements⁽¹¹⁾ which have shown that deuterium increases the phonon frequencies in both the longitudinal and transverse acoustic phonon branches of the dispersion curves for b.c.c. metals. The increased phonon frequencies despite the very large volumes of solution, suggest increases in the lattice force constants due to the deuterium rather than the decreases postulated in the "decohesion" model. Caglioti et al⁽¹²⁾ have related the fracture surface energy to the longitudinal phonon frequency at the Brillouin Zone boundary. The increases in these frequencies which are observed on alloying Nb with deuterium suggest an increase in atomic bond strength and surface energies and therefore indicate that the observed embrittlement is not related to weakening of atomic bonds.

It is also unlikely that the high temperature embrittlement can be accounted for by solid solution strengthening i.e. by an increase in "notch sensitivity." Only a small increase in yield strength is observed as the hydrogen concentration is increased (Fig. 5) and in the lower concentrations no increase occurs. This is in contrast to solid solution strengthening which is usually manifested at the low concentrations. Since

the high hydrogen diffusivity allows solute atmospheres to drift along with moving dislocations at velocities as high as two meters/sec⁽¹³⁾ atmospheres cannot serve as effective dislocation obstacles. Moreover, Nb specimens strengthened by cold work had the same fracture behavior as well annealed specimens (Fig. 1) suggesting that solid solution strengthening is not the direct cause of the high temperature embrittlement observed.

The general fracture behavior observed in the high temperature Nb-H alloys can be accounted for by the stress induced precipitation and cleavage of $\gamma(\text{NbH}_2)$ hydride at the advancing crack front in a manner analogous to the mechanism described^(2,3) for the low temperature fracture behavior of Nb-H alloys. In this mechanism, cleavage occurs and terminates the plastic deformation of the alloy when a stress induced brittle hydride forms and undergoes cleavage. This occurs at a stress concentration which may result from notches or dislocation pileups and at a rate which is determined by diffusion of the hydrogen to the stress concentration. Crack propagation occurs by repeated formation and cleavage of the hydride. The thermodynamics of the equilibrium between the solid solution and the hydride is affected by the stress field at the crack tip with tension stresses increasing the hydride solvus temperature. The strain to failure reflects the temperature and flow stress since plastic flow followed by ductile fracture will occur unless the hydride is formed. On the basis of this mechanism, the ductile - cleavage transition corresponds to the hydride solvus temperature under

the stress field at the crack tip. (2,3)

At elevated temperatures two hydrides can form from the α' solid solution and give rise to embrittlement, the β phase centered around NbH and the γ phase centered around NbH_2 . The f.c. orthorhombic β phase forms from the α' phase with about a 2% volume increase. (14,15) The γ hydride has a cubic fluorite structure and forms from the α' with about 20% increase of the molal volume at 200 C. (14,15) The influence of an external tensile stress on the equilibrium between the α' solid solution and the β and γ hydrides can be calculated by applying the thermodynamics of stressed solids (16) as discussed for the α - β equilibrium. (17) Using the approach of Birnbaum et al. (17) stress induced increases in the $\alpha' \rightarrow \beta$ solvus temperatures can be estimated to be about 25 C for a biaxial tensile stress of $\mu/30$. This increase is considerably smaller than the observed difference between the experimentally observed $\alpha' \rightarrow \alpha' + \beta$ solvus under zero external stress and the curve which bounds the ductile-brittle transition (Fig. 1). It therefore appears that stress induced β hydride cannot account for the high temperature fracture transition.

Since the $\alpha' - \gamma$ transition is accompanied by a much greater volume increase than the $\alpha' - \beta$ transition it is expected to exhibit much greater increases of the observed solvus temperatures with external stress. (17) Applying the thermodynamics of stressed solids to the $\alpha' - \gamma$ equilibrium results in the following expression for the increase in solvus temperatures due to the reversible work done by an external biaxial stress field:

$$\Delta T = T_S^{\sigma} - T_S^{\circ} = \frac{2\sigma \Delta V}{3R(\Gamma - \ln C_H)} \quad (1)$$

where σ is the principal normal stress, ΔV is the molal volume increase on forming the γ hydride from the α' solid solution, C_H is the mole fraction of the hydrogen, Γ is the activity coefficient of H in α' and T_S° and T_S^{σ} are the $\alpha' - \gamma$ solvus temperatures for the constrained hydride under zero stress and under a biaxial tension stress field. If α' is assumed to be an ideal solution the solvus temperatures which result from this calculation are shown in Fig. 6 for an external stress of $\mu/30$.

The derivation of Eqn. 1 assumes that the elastic and plastic accommodation processes are not affected by the external stress. In addition to the increase in the solvus temperature given by Eqn. 1, the stress can also decrease the accommodation free energy by aiding the formation and motion of the prismatic dislocations necessary to accommodate the molar volume increase. (17) This non-equilibrium effect can further increase the observed solvus temperature towards T_e° , the equilibrium solvus temperature for the unconstrained hydride under stress. This temperature is the upper limit for the stability of the γ hydride under stress. The free energy of these elastic and plastic accommodation terms can be estimated by: (17)

$$\Delta G_{\text{ACCOM}} = \frac{2\mu}{3\alpha} \frac{\Delta V^2}{\bar{V}} \simeq 2200 \text{ cal/mole}, \quad (2)$$

where $\alpha = 1 + \frac{4\mu}{3\beta}$, μ = shear modulus, β = bulk modulus,

ΔV = molar volume change on forming γ from α' , and \bar{V} is the molar volume of the α' solid solution. The free energy of formation of the constrained γ in the absence of stress can be estimated from the observed $\alpha' - \gamma$ solvus to be about 1800 cal/mole and therefore the total free energy change at the $\alpha' \rightarrow \gamma$ transition in the absence of any volume constraints is $\Delta G_{TOT}^{\alpha' \rightarrow \gamma} \cong 4000$ cal/mole. The equilibrium solvus temperatures for unconstrained γ in equilibrium with α' , T_e^0 , can be determined from the following expression:

$$\Delta G^{\alpha' \rightarrow \gamma} \cong 4000 \text{ cal/mole} = 2RT_e^0 \ln(\Gamma C_H) \quad (3)$$

and are shown in Fig. 6 as are the equilibrium unconstrained solvus temperatures under a biaxial tension stress of $\mu/30$, T_e^σ , which are calculated from Eqn. 1.

The α' is metastable between T_S^0 and T_e^0 at zero stress. The application of an external tensile stress increases both of these solvus temperatures an equivalent amount to T_S^σ and T_e^σ . Since the external stress does not decrease the accommodation free energy terms completely, the observed solvus temperature will lie between T_S^0 and T_e^σ . The experimentally observed ductile - cleavage transition temperature lies between T_S^0 and T_e^σ as shown in Fig. 6. Therefore the phase field which corresponds to the observed cleavage fractures lies within the region in which γ hydride can be formed under an applied tensile stress and the fracture transition temperature can be considered to be the solvus temperature under stress, T_S^σ . The increasing difference be-

tween the ductile - cleavage transition temperature, which corresponds to T_S^0 , and T_e^0 above 400°C may result from the decreasing yield strength with increasing temperature since T_S^0 depends on stress. The stresses attained prior to ductile rupture are expected to decrease as the test temperature is increased.

The fracture behavior observed in Nb-H alloys at elevated temperatures can be accounted for by stress induced γ hydride at the advancing crack front in a mechanism similar to that shown^(2,3) to account for the low temperature embrittlement. This fracture mechanism suggests that at test temperatures below T_e^0 the γ phase can be formed at stress concentrations due to the effects of external stress on the $\alpha \rightarrow \gamma$ phase equilibria. The γ hydride is known to be a brittle phase⁽¹⁵⁾ which therefore cleaves after precipitation. The process is then repeated at the new crack front and the cleavage crack propagates at a rate which is controlled by diffusion of hydrogen to the crack tip and the formation of the γ hydride.

The isothermal concentration dependence of the fracture behavior at 300°C can be accounted for by this model. At C_1 (Fig. 6), $T > T_e^0$ so that stress induced precipitation of γ cannot occur prior to ductile failure. At a concentration such as C_2 , $T_e^0 > T > T_S^0$ at the maximum stress reached during deformation and ductile failure again follows. At $C > C_3$, $T < T_S^0$ at the stresses attained prior to ductile fracture and precipitation of γ followed by its cleavage occurs leading to cleavage fracture after plastic deformation. Since work hardening is required to reach the stress to form γ , the strain prior to cleavage failure will decrease as C_H is increased and the undercooling ($T_e^0 - T$)

increases. The strain prior to fracture will also decrease as a result of the increased flow stress which accompanies increasing hydrogen concentration and from any other solution strengthening. A similar sequence of behavior can be observed on decreasing the test temperature at constant C_H . Thus the experimentally observed behavior is consistent with this mechanism. Cleavage fracture due to the stress induced precipitation of the γ phase is expected to be relatively continuous and rapid as a result of the high hydrogen diffusivity in these alloys ($D \approx 2 \times 10^{-5} \text{ cm}^2/\text{sec.}$).⁽¹⁸⁾ Once a stress which is sufficient to stabilize the γ phase is achieved, the macroscopic ductility will be terminated by continuous precipitation and cleavage of γ at the advancing crack tip. The observed $\{110\}$ cleavage planes should correspond to γ hydride cleavage plane.

The temperature and concentration dependence of the yield strength (Fig. 5) is also consistent with the stress induced γ hydride formation. The increased yield stress in the temperature-composition range which is characterized by cleavage fracture may be due to γ precipitates which form in the tension stress field of dislocations and act as effective pinning points to dislocation motion.⁽¹⁹⁾

5. CONCLUSIONS

The Nb-H alloys having compositions $H/Nb \gtrsim 0.3$ were shown to fail in a cleavage mode at temperatures less than 450°C. The strain to failure decreased as the temperature decreased and as H/Nb increased. Measurements of the fracture surface energy of the alloys which failed by low ductility cleavage gave values

which were typical of b.c.c. metal surface energies. Hydrogen in solid solution does not appear to decrease the effective surface energy of the niobium.

The experimental results were accounted for by a stress induced hydride fracture mechanism. In the high temperature range it was shown that the hydride associated with the fracture was most likely to be the γ NbH₂ hydride and that it could be stress induced over the temperature and composition ranges in which cleavage fracture was observed.

REFERENCES

1. H. K. Birnbaum, M. L. Grossbeck, and S. Gahr: Hydrogen in Metals (American Society for Metals, Metals Park, OH, 1974), p. 203.
2. S. Gahr, M. L. Grossbeck, and H. K. Birnbaum: Acta Met., 25, 125 (1977).
3. M. L. Grossbeck and H. K. Birnbaum: Acta Met., 25, 135 (1977).
4. R. J. Walter: Research Report RR 64-6 Rocketdyne, Canoga Park, CA, (1964).
5. R. J. Walter and W. T. Chandler: Trans. AIME, 233, 762 (1965).
6. A. R. Troiano: Trans. ASM, 52, 54 (1960).
7. R. A. Oriani: Ber. der Bunsenges. fur Phys. Chem., 76, 848 (1972).
8. R. A. Oriani and P. H. Josephic: Scripta Met., 6, 681 (1972).
9. J. C. Liu and J. C. Bilello: (to be published).
10. T. C. Lindley and R. E. Smallman: Acta Met., 11, 367 (1963).
11. J. M. Rowe, N. Vagelatos, and J. J. Rush: Phys. Rev. B, 12, 2959 (1975).
12. G. Caglioti, G. Rizzi, and J. C. Bilello: J. App. Phys., 42, 4271 (1971).
13. A. H. Cottrell: Dislocations and Plastic Flow in Crystals, Oxford Press, p. 136 (1953).
14. W. M. Albrecht, M. W. Mallett, and W. D. Goode: J. Electrochem. Soc., 105, 219 (1958).
15. J. J. Reilly and R. H. Wiswall: Inorg. Chem., 9, 1681 (1970).
16. J. C. M. Li, R. A. Oriani, and L. S. Darken: Z. Phys. Chem., New Folge, 49, 271 (1966).
17. H. K. Birnbaum, M. L. Grossbeck, and M. Amano: Journ. Less-Common Metals, 49, 357 (1976).
18. J. Völkl and G. Alefeld, Diffusion in Solids: Recent Developments (Academic Press N.Y.) ed. by J. J. Burton and A. S. Nowick (1975) Chap. 5.

19. C. C. Chen and R. J. Arsenault: Hydrogen in Metals
(American Society for Metals, Metals Park, OH, 1974).

Fig. 1. Strain to failure vs temperature and composition for the high temperature alloys. The data are superimposed over the Nb-H phase diagram (after Walter and Chandler Ref. 5). The dotted line (....) indicates the ductile - cleavage fracture transition. The type of fracture morphology observed is indicated at each data point with (G) denoting ductile failure and (O) denoting cleavage. (Δ) denotes ductile failure and (V) denotes cleavage in cold worked niobium specimens; (+) denotes ductile failure and (*) denotes cleavage in deuterium doped specimens. The percent strain to failure is given next to each data point. N.M. indicates the strain to failure was not measured. All tests were run at $\dot{\epsilon} = 5 \times 10^{-4} \text{ sec}^{-1}$.

Fig. 2. Fracture surfaces of niobium-hydrogen alloys tested at 300 C. The fractographs are from specimens tested at compositions of (a) $\text{NbH}_{0.26}$, (b) $\text{NbH}_{0.30}$, (c) $\text{NbH}_{0.71}$ and (d) $\text{NbH}_{0.93}$, at $\dot{\epsilon} = 5 \times 10^{-4} \text{ sec}^{-1}$.

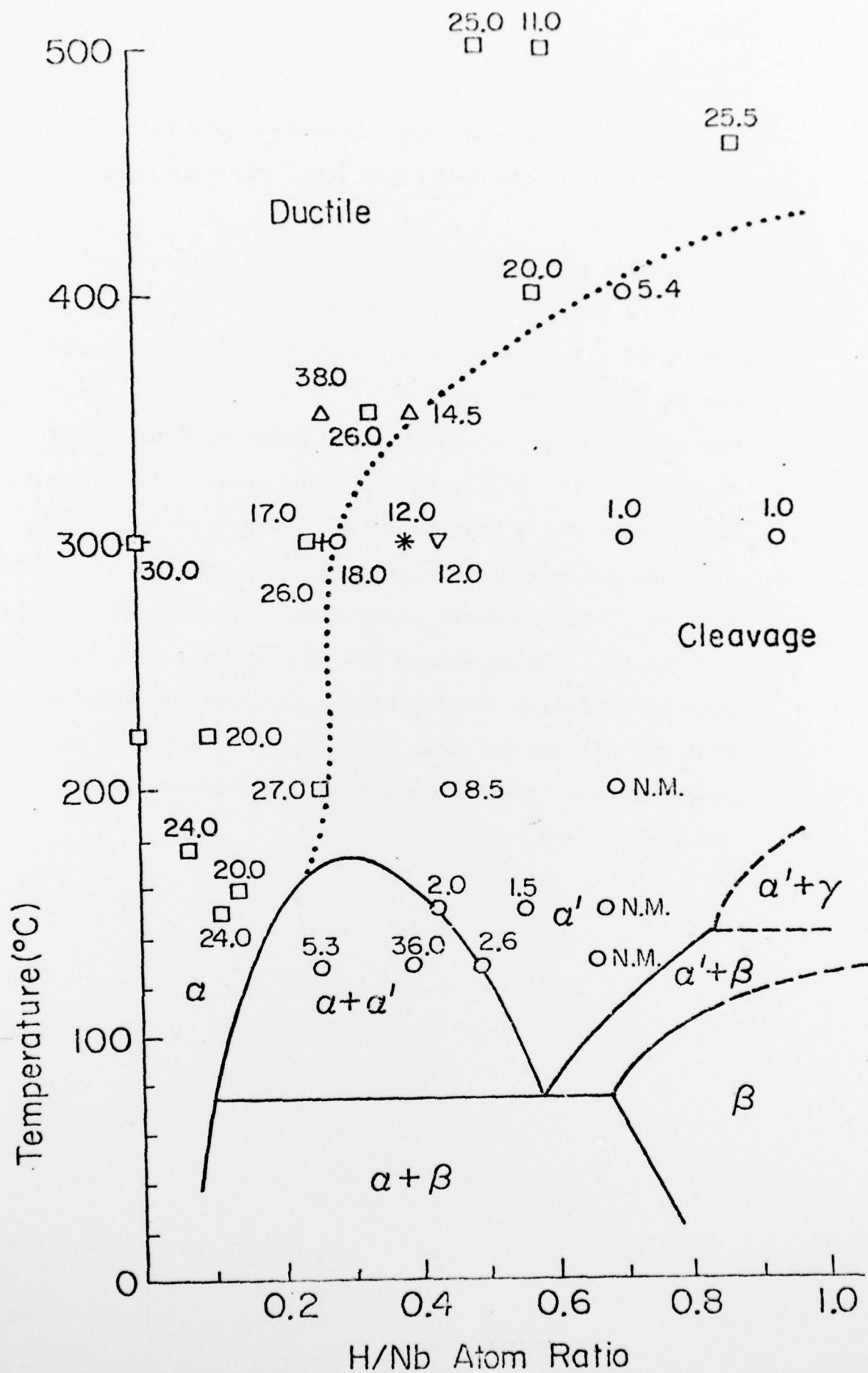
Fig. 3. Fracture surface of niobium-hydrogen alloys tested at a composition of $\text{NbH}_{0.70}$. The fractographs are from specimens tested at (a) 130 C, (b) 150 C, (c) 200 C, (d) 300 C, (e) 400 C and (f) 450 C, at $\dot{\epsilon} = 5 \times 10^{-4} \text{ sec}^{-1}$.

Fig. 4. Fracture surfaces of $\text{NbH}_{0.82}$ single crystals tested at 138 C within the α' phase. The fracture planes shown are the (a) $\{110\}$ and (b) $\{100\}$. The arrows indicate the position of the spark eroded precrack. Electron channel-

ling patterns made near the notch root are shown in (c) and (d) for the $[110]$ and $[100]$ fracture planes, respectively.

Fig. 5. The tensile yield strength of the high temperature alloys vs temperature and composition. The test temperature is indicated for each curve. Tests were run at $\dot{\epsilon} = 5 \times 10^{-4} \text{ sec}^{-1}$.

Fig. 6. The effect of stress on the Nb-H phase diagram in the vicinity of the $\alpha' + \gamma$ solvus. The equilibrium solvus temperature for γ hydride in the absence of volume constraints was calculated using Eq. (3) and is shown as $(-\cdot-\cdot-)$. The increase in both the experimental solvus and the equilibrium solvus due to the reversible work done by a biaxial tensile stress of $\mu/30$ was calculated from Eq. (1) and is shown as $(- --- -)$ and $(-----)$, respectively. The cleavage fracture transition is shown as $(\cdot\cdot\cdot\cdot)$.





100 μm

B



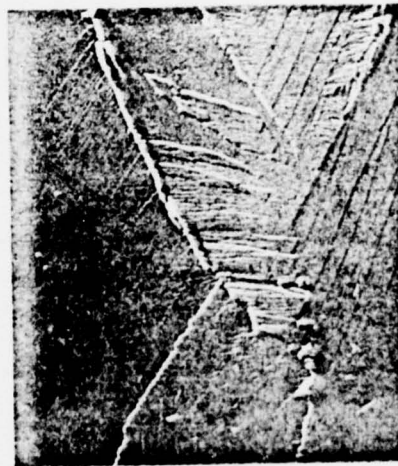
100 μm

D



10 μm

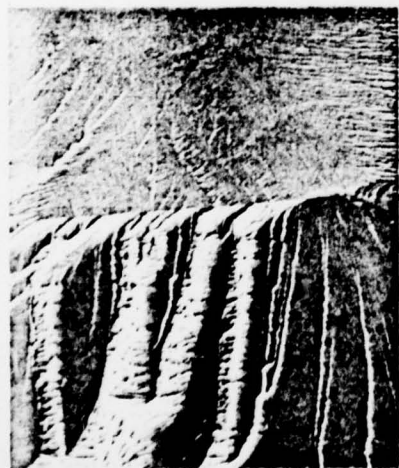
A



100 μm

C

Gahr & Birnbaum FIG 2



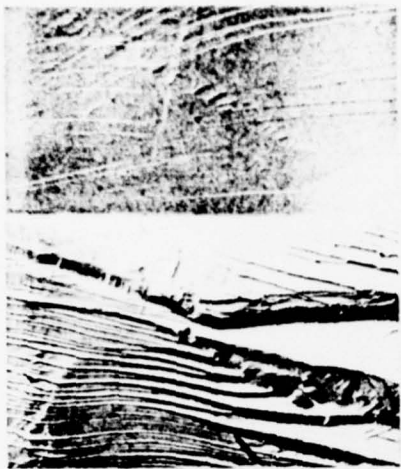
100 μm

A



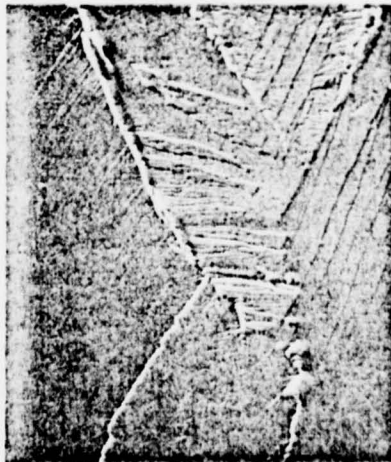
100 μm

B



100 μm

C



100 μm

D



10 μm

E



100 μm

F

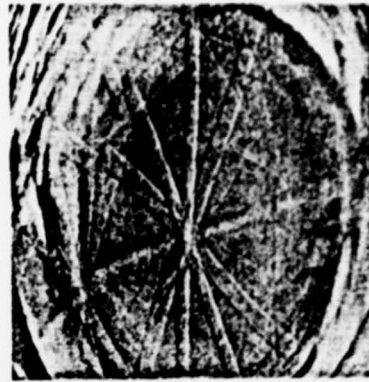
Gahr + Birnbach FIG 3



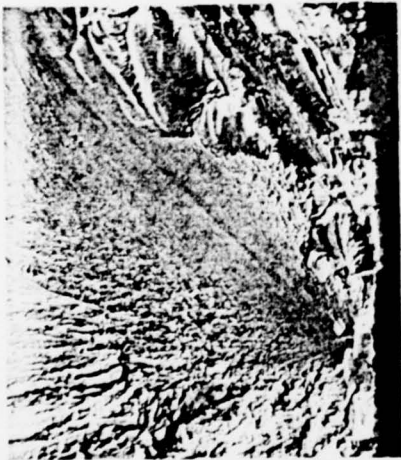
100 μ m



A



B



100 μ m

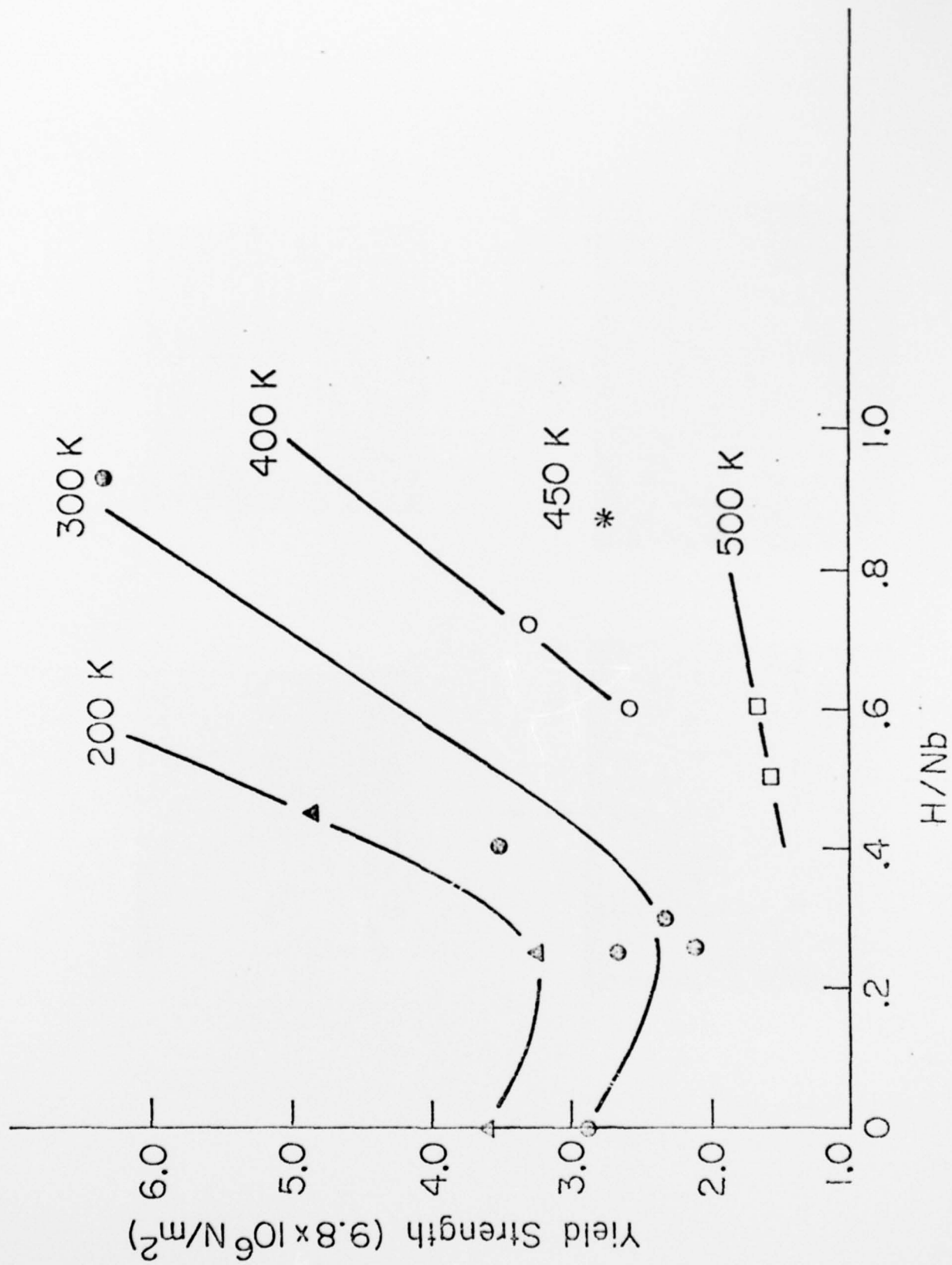


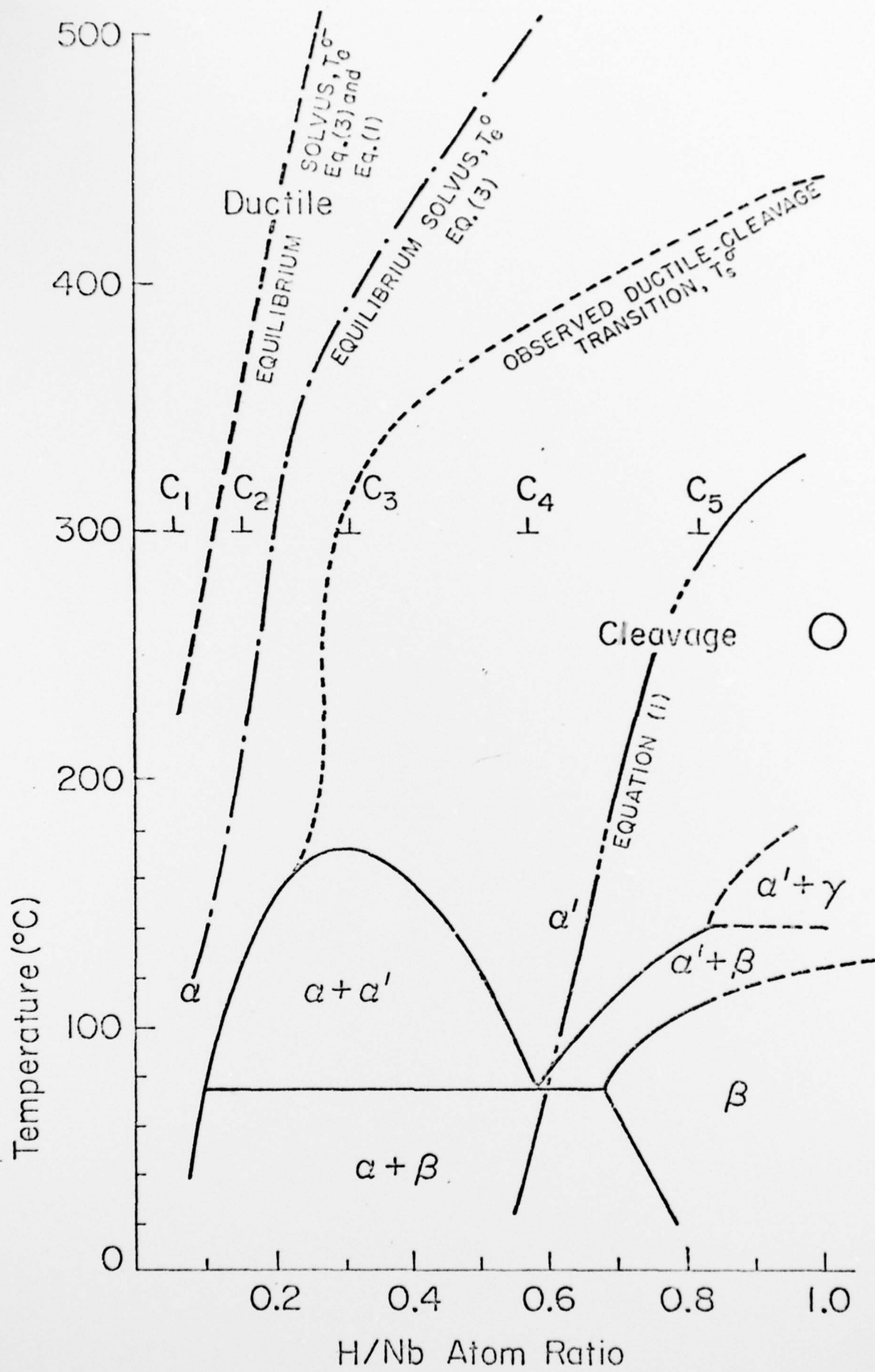
C



D

Gahr & Birnbaum Fig 4





Unclassified

Security Classification

DOCUMENT CONTROL DATA - R & D

Security classification of title, body of abstract and indexing annotation must be entered when the overall report is classified.

ORIGINATING ACTIVITY (Corporate author)

University of Illinois

2a. REPORT SECURITY CLASSIFICATION

UNCLASSIFIED

2b. GROUP

REPORT TITLE

(6) Hydrogen Embrittlement of Niobium III - High Temperature Behavior.

A. DESCRIPTIVE NOTES (Type of report and, inclusive dates)

(9) Technical Report.

1. AUTHOR (Last name, middle initial, first name)

Gahr, S. and Birnbaum, H. K.

(10) S./Gahr H.K./Birnbaum

6. REPORT DATE

October 18, 1977

(11) 18 Oct 77

7a. TOTAL NO. OF PAGES

25

7b. NO. OF REFS

19

8. CONTRACT OR GRANT NO.

(15) N 00014-75-C-1012

9a. ORIGINATOR'S REPORT NUMBER(S)

(12) 320

b. PROJECT NO.

c.

9b. OTHER REPORT NO(S) (Any other numbers that may be assigned this report)

d.

10. DISTRIBUTION STATEMENT

This document is unclassified. Distribution and reproduction for any purpose of the U. S. Government is permitted.

11. SUPPLEMENTARY NOTES

12. SPONSORING MILITARY ACTIVITY

Office of Naval Research

13. ABSTRACT

The deformation behavior in niobium-hydrogen alloys was investigated in the temperature range 125 - 500 C and at compositions up to H/Nb of 0.9. High temperature tensile tests and fractographic studies were applied to determine the fracture mechanisms. It is shown that at $T \lesssim 450$ C and $H/Nb \gtrsim 0.3$ fracture occurs by a cleavage mode. The mechanism of this high temperature hydrogen embrittlement is discussed. The fracture mechanism is shown to be consistent with the stress induced formation and cleavage of NbH_2 .

176 $\phi 14$ < $\sigma_1 =$

Gahr

DL FORM 1473 (PAGE 1)

S/N 01. 107-6811

UNCLASSIFIED

Security Classification

A-31408

Security Classification

S/N 0101-807-88-1

Security Classification

A - 31409



10 μm

A



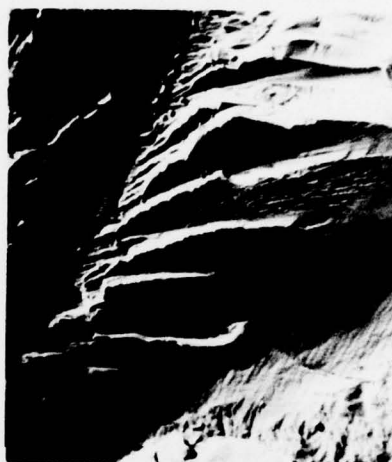
100 μm

B



100 μm

C



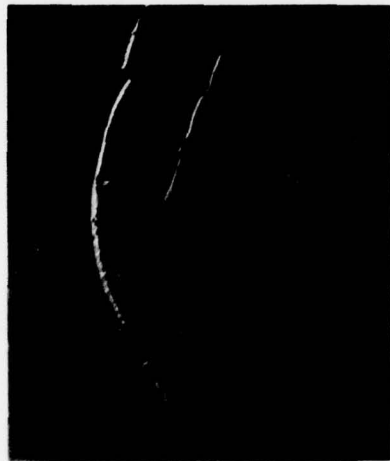
100 μm

D



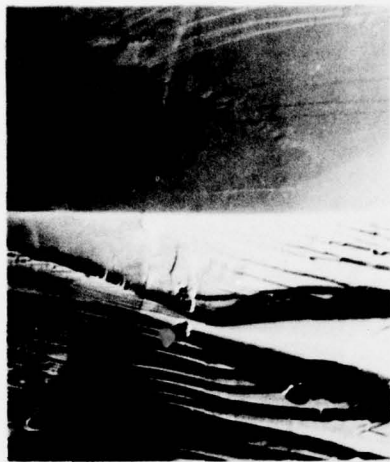
100 μm

A



100 μm

B



100 μm

C



100 μm

D



10 μm

E



100 μm

F



100 μ m



B



D



100 μ m



A



C

Gahr & Birnbaum Fig 4